Using proximal soil sensors and fuzzy classification for mapping Amazonian Dark Earths

Mats Söderström[1], Jan Eriksson[2], Christian Isendahl[3], Suzana Romeiro Araújo[4], Lilian Rebellato[5], Denise Pahl Schaan[6] and Per Stenborg[3]

[1]Department of Soil and Environment, Swedish University of Agricultural Sciences, Box 234, SE-532 23 Skara, Sweden.

[2]Department of Soil and Environment, Swedish University of Agricultural Sciences, Box 7014, SE-750 07 Uppsala, Sweden.

[3]Department of Historical Studies, University of Gothenburg, Box 200, SE-405 30, Gothenburg, Sweden.

[4]Department of Soil Science, Universidade de São Paulo, CP 09, 13418-900, Piracicaba, SP, Brazil.

[5]Department of Anthropology and Archaeology, Universidade Federal do Oeste do Pará, Rua Vera Paz s/n, Salé 68040-250, Santarém, PA, Brazil.

[6]Programa de Pós-Graduação em Antropologia, Universidade Federal do Pará, Rua Augusto Correa 1, CEP 66075-110, Belem, PA, Brazil.

e-mail: mats.soderstrom@slu.se

We tested if hand-carried field proximal soil sensing (PSS) can be used to map the distribution of anthropogenic Amazonian Dark Earths (ADE). ADE soils are rich in archaeological artefacts, nutrients, organic matter and carbon in the very stable form of pyrogenic carbon, also referred to as black carbon or biochar. To test the capacity of PSS to detect signature ADE properties we measured electrical conductivity (ECa), magnetic susceptibility (MSa) and gamma ray data by transect sampling and compared these readings, using fuzzy classification, with datasets on chemical soil properties from a 28 ha large study area located on the Belterra Plateau of the Lower Amazon in northern Brazil. Results indicate that ECa and MSa measurements were good indicators of ADE signatures, but that the gamma radiation sensor was less useful in the strongly weathered soils. PSS and fuzzy classification can be used for rapid field mapping of ADE for both agricultural and archaeological purposes.

Key words: Electromagnetic induction, magnetic susceptibility, gamma radiation, anthropogenic soil types, prehistoric agriculture, archaeology

Introduction

The potential of Amazonian Dark Earths (ADE) as a valuable resource for agriculture and as a key source for understanding the prehistory of the Amazonian cultural landscape has been recognized for some time (Sombroek 1966, Smith 1980). The focused multidisciplinary investigation of this phenomenon took off during the 2000s (e.g. Lehmann et al. 2003, Glaser and Woods 2004, Woods et al. 2009, Glaser and Birk 2012) and suggests that ADEs formed through the deposition of organic material from domestic and agricultural activities during the prehistoric period. A particularly important land use practice contributing to ADE formation is 'slash and char' agriculture in which burning with reduced supply of oxygen transforms part of the biomass to pyrogenic carbon through pyrolysis, supplemented by the addition of other kinds of organic material associated with long-term concentrated settlement. ADEs are rich in archaeological artefacts (e.g. ceramics and lithics), nutrients such as phosphorus (P), calcium (Ca) and magnesium (Mg), organic matter and carbon (C) in the very stable form of pyrogenic carbon, and is a unique agricultural and archaeological resource distinct from the strongly weathered soils that dominate in the Amazon region. While organic matter normally decomposes rapidly under tropical climatic conditions, pyrogenic carbon is resistant to disintegration and increases the long-term nutrient-holding capacity of the soil.

ADEs are often referred to as *terra preta* and *terra mulata* (e.g. Kämpf et al. 2003). The former is blackish in colour and rich in archaeological artefacts, nutrients and pyrogenic C. *Terra mulata* is primarily distinguished from surrounding natural soil by darker colour of the surface horizon due to higher C content and occurrence of pyrogenic carbon, and is commonly interpreted as resulting from less intensive agriculture (Sombroek 1966, Woods and McCann 1999).

Manuscript received May 2013

In soil descriptive terms ADEs have an anthropogenic A horizon and can according to Kämpf et al. (2003) be classified as Fimic Anthrosols (FAO 1988) and Plaggic or Hortic Anthrosols (WRB 2006). ADE remains the most important resource for smallholder agriculture in the Amazon region and is a demonstrably sustainable resource under low-intensive farming. Furthermore, several aspects of ADE formation and management are not only regionally relevant but have universal applications. In particular, the principles of ADE formation and the benefits of high amounts of pyrogenic C have become key issues for research on carbon sequestration and long-term soil fertility globally (Lehmann and Joseph 2009, Verheijen et al. 2010).

ADEs occur in patches ranging in size from less than a hectare to a few hundred hectares. Their known distribution is concentrated along the main rivers and tributaries of the Amazon watershed, but mapping is still in its infancy and regional and local distribution maps are usually strongly fragmentary owing to logistical issues and the size of the region. In recent years, digital soil mapping has evolved as a cost-efficient approach to predict spatial patterns of soil properties across geographical scales by integrating quantitative methods with proximal and remote sensing, soil observations and other covariates such as digital elevation data (Grunwald 2010). This type of technique is of particular interest in areas, such as the Amazon, where the available information on land quality and soil resources that guides land-use planning decisions is fragmentary (Fearnside and Leal Filho 2001, Teixeira et al. 2008). Proximal soil sensing (PSS; sensors used in close contact with or within a few meters distance from the measured soil) is a way to rapidly and often non-destructively collect detailed information on the soil surface or of a given soil volume (Viscarra Rossel and McBratney 1998). PSS instruments record the energy emitted from the soil in different parts of the electromagnetic spectrum (Adamchuk and Viscarra Rossel 2013).

The aim of the study reported here was to investigate if hand-carried field soil sensors can be used to map the extent of patches of ADE. To test the capacity of PSS to detect signature properties we measured electrical conductivity, magnetic susceptibility and gamma ray data by transect sampling and compared these readings with datasets on chemical soil properties. If successful, test results will indicate that PSS applications can be a mapping tool of ADE for both agricultural and archaeological purposes.

Materials and methods

Study area

The 28-ha large study area is located at Bom Futuro on the Belterra Plateau, ca. 40 km south of the city of Santarém in the state of Pará, Brazil (Fig. 1). The Santarém area is a principal region for the occurrence of ADE (Nimuendajú 2004, Stenborg 2009, Woods et al. 2009), as well as the place of original discovery and description of this phenomenon (Hartt 1874). Archaeological remains at Bom Futuro were first reported by Nimuendajú in the 1920's (Nimuendajú 2004). The area includes significant soil variation in a partly cultivated partly forested landscape, covering both known (and possibly unknown) patches of ADE as well as non-anthropogenic Ferralsols. Archaeological excavations in the southwest sector of the study area (Fig. 1) suggest that permanent settlements had been established at this location at least by the late prehistoric period and occupied the area into the early contact period, ca. 14th–17th centuries AD (Stenborg and Bakunic 2011, Stenborg et al. 2012). The Belterra Plateau is an upland (*terra firme*) environment elevated ca. 150 m above the Amazon and Tapajós river floodplains (*várzea*). The annual precipitation on the plateau is 1920 mm on average and the annual average temperature 25–28 °C (data from INMET, Brazil). Geologically, the Belterra Plateau forms part of the Cretaceous Alter do Chão Formation. The clayey soils in the Central and Lower Amazon have a homogenous composition and frequently consist of more than 80% kaolinite. Other minerals are quartz and to a lesser extent anatase and gibbsite (Irion 1984). The clay soils in the study area can thus be expected to contain few weatherable minerals that can release nutrients such as Ca, potassium (K), Mg and sodium (Na) and local vegetation depends on rapid biomass cycling. Texture data from six soil profiles studied at Bom Futuro within our project indicate a clay content in the range of 70–90% (Araújo 2012).

Smallholder households at Bom Futuro practice low-intensive, long-fallow slash-and-burn shifting cultivation of manioc, maize and other cultivars that results in a local mosaic, from recently cleared patches to very dense forest at various stages of regrowth. Shrub and medium-high forest dominate. Regrowth includes a number of wild and introduced domesticated plants, e.g. Brazil nut (*Bertholletia excelsa* Humb. & Bonpl.), avocado (*Persea americana* Mill.), mango *(Mangifera indica* L.*)* and cacao (*Theobroma cacao* L.). Three ha in the southeastern corner of the study area have been converted into an arable field, which extends eastwards and mainly produces soybean. A smallholder farmer's residential homestead is located in the northeastern section of the study area, covering about 2 ha, and the soil cover there is affected by various domestic activities. Another smallholder homestead is located just outside the northwestern limit of the Bom Futuro study area.

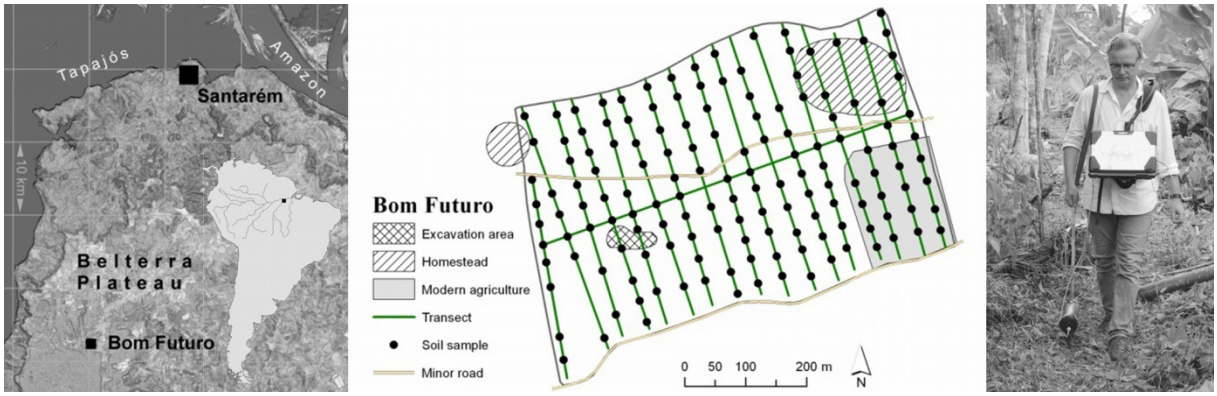

Fig. 1. Location and general outline of the Bom Futuro survey area, 40 km south of Santarém, in Pará, Brazil. The photo shows transect scanning with a field sensor.

Soil sampling

A system of sampling transects were laid out in order to carry out soil investigations in the often dense vegetation. From a central 640 m long ENE-WSW transect cleared through the forest, perpendicular transects were cleared 200 m in both directions every 40 m along the base transect (Fig. 1). Soil samples (0–20 cm) were taken with an auger at sample points located every 40th meter along transect lines (Fig. 1). At each sampling point (n = 148), a composite sample of three cores was obtained in a triangle with a side length of ca. 1 m and the depth of the part of the core that was A-horizon was noted.

Chemical analyses

The following analyses were made on the soil samples: pH measured in a soil:water solution ratio of 1:2.5; soil organic carbon (SOC) content determined by wet oxidation with K-dichromate with a modified Walkley & Black method (EMBRAPA 2009); extractable P by Mehlich 1; exchangeable calcium (Ca^{2+}), potassium (K^{+}), magnesium (Mg^{2+}) and aluminium (Al^{3+}) extracted with 1 M KCl (EMBRAPA 2009) and analysed with atomic absorption spectrophotometry; and exchangeable acidity (H^{+}+ Al^{3+}) extracted with 1 M calcium acetate at pH 7. Exchangeable acidity was determined volumetrically by a back-titration of the acetate extract with NaOH in the presence of phenolphthalein as an indicator. Cation exchange capacity (CEC, at pH 7) and base saturation were calculated from the analyses of base cations and exchangeable acidity.

Sensor measurements

Two handheld sensors were used: the EM38-MK2 (Geonics Ltd., Mississauga, Canada) and the Mole (the Soil Company, Groningen, Netherlands). The former outputs the apparent soil electrical conductivity (ECa in mS m^{-1}) at two depths simultaneously (mainly 0–0.5 m and 0–1.0 m effective depth, respectively), as well as values proportional to the apparent magnetic susceptibility (MSa; with an effective depth of about half that of ECa). In this report only the values of ECa and MSa from the lower depth were used owing to instability in sensor registrations for the upper depth. Instruments measuring electromagnetic induction (EMI) have been used in soil surveys for many years and proved useful for mapping soil properties such as salinity, soil water content and clay content (Corwin and Lesch 2003), also in archaeological research (e.g. Clay 2006). The gamma ray sensor records the natural occurrence of the radioactive isotopes ^{238}U (uranium), ^{232}Th (thorium), ^{40}K (potassium), ^{137}Cs (cesium) and TC (total counts in the decay per second) in the topsoil (ca. 0.3 m soil depth). The gamma ray emission of the soil is affected by the soil parent material as well as weathering processes (IAEA 2003). PSS of gamma radiation with this instrument has been successfully applied in studies of soil clay content and heavy metal concentrations (van der Klooster et al. 2011, Piikki et al. 2013, Söderström and Eriksson 2013). At Bom Futuro both instruments were carried by hand about 15 cm above ground along transects (Fig. 1) and measurements were made continuously every second. The position of each measurement was logged simultaneously; the position of the EM38 was registered by a TDS Nomad GPS (Tripod Data Systems, Corvallis, OR, USA) and the gamma sensor by a Bu-353 GPS (GlobalSat, New Taipei City, Taiwan). The EM38 instrument was used in the vertical position. The Soil Company extracted the radioelement concentrations in Bq kg^{-1} from the scanned gamma-ray spectra using full-spectrum analysis (Hendriks et al. 2001). The ten observations nearest a soil sampling site were averaged for mapping and comparison with soil chemical analyses.

Mapping and statistical analyses

Geostatistics was used for spatial description and mapping of sensor data and soil properties. It is a stochastic technique based on establishing the autocorrelation between observation points avoiding dependence upon the mean (Isaaks and Srivastava 1989). In order to establish the autocorrelation between observation points, the measured value *V* at a location *x* of a single variable *Z* is described in terms of the distance of separation (lag distance *h*) between observation points. This is given by the semivariance γ, which is the average square of the difference in value of *V* between all pairs *n* of observations a given *h* apart. The sample variogram ($\gamma^*_{(h)}$) is calculated as follows:

$$\gamma^*_{(h)} = \frac{1}{2n}\sum_{i=1}^{n}(V(x_i) - V(x_{i+h}))^2 \quad (1)$$

and plotted against *h* in a so-called experimental variogram. A model variogram, whose shape and type determines the interpolation weights was then fitted to the computed sample variogram. The behaviour of the model near the origin (the nugget variance C_0) is the most crucial for interpolation, together with the overall variance (sill = C_0 + partial sill *C*) and the distance over which the semivariance continues to increase in magnitude (the range *R*). These model parameters were used for interpolation $Z^*_{(x)}$ by ordinary block kriging. Mapping and geostatistics were performed using ArcGIS 10.1 with the extensions Spatial Analyst and Geostatistical Analyst (ESRI Inc., Redlands, CA, USA).

Fuzzy *k*-means were used in order to merge and classify the sensor data in the research area, the disturbed areas of the homestead and arable field exempted. In many types of classifications, each location is given a single class according to some determined criteria, even though it may be difficult to determine to which class some locations should belong. As an alternative the method used here is based on a *continuous* classification, i.e. that every location can belong to any class to some extent with a value of likelihood called a membership value (MF) ranging from 0 (no membership) to 1 (maximum membership). This results in a set of *k* continuous classes (or clusters) in attribute space that minimizes the within-class sum square errors (see Burrough and McDonnell 1998). Before performing the fuzzy classification, the data from each sensor were standardized by subtracting the mean and dividing by the standard deviation, producing an estimated Z-score. The Z-scores were then imported in the FuzME software (Minasny and McBratney 2002) to compute the fuzzy *k*-means for different numbers of classes (*k* = 3–7) and with different fuzzy exponents *q* (set to 1.3–1.7). To determine the optimal number of classes, the combination (*k*, *q*) with the lowest fuzzy performance index (FPI) was selected. FPI values close to 1 indicate significant overlaps while values approaching 0 show that the classes are more distinct, which is assumed to represent a better classification.

Results

Soil chemistry

Geochemical analyses demonstrated that there was great diversity in soil properties over the research area (Table 1). The more or less natural soil in the arable field was classified according to the World Reference Base for Soil Resources (WRB 2006) as an Acric Vetic Ferralsol (Hyperdystric, Clayic, Xantic), based on chemical data and soil profile descriptions presented in Araújo (2012). The soil profile at one of the most typical ADE locations in one of the archaeological excavations was classified as Ferralic, Hortic Anthrosol (Endodystric, Clayic). Interpolated maps of some of the soil properties are shown in Figure 2.

In the Bom Futuro research area the concentration of soil organic carbon in the upper 20 cm of the soil is on average 23 g kg^{-1}. Eighty per cent of the values are in the range of 18–30 g kg^{-1}. Concentrations in the lower part or below this range were found in the eastern part of the area, which is affected by homestead domestic activities and modern cash crop production. At the homestead, litter is continuously swept from the ground by residents. The soil surface is also hardened by trampling, which further promotes the removal of loose organic litter by wind action. The lower C content in the arable field is probably a result of the effect of tillage, which promotes decomposition. Harvest of biomass also promotes lower soil C content unless compensated for by an increased production of roots and crop residues due to fertilization. The highest organic C concentrations are found in the sector where prehistoric and early historic settlement remains were excavated and in the kitchen garden plots of the homestead in the northwestern part of the area.

Table 1. Summary statistics of soil properties (0–20 cm depth) at Bom Futuro (n = 148).

Soil property	Mean	Min	25%-per-centile	Median	75%-per-centile	Max*
A-horizon depth (cm)	9	0	5	8	12	20
SOC (g kg^{-1})	23	10	20	23	26	38
pH-H_2O	5.0	4.0	4.6	4.9	5.3	6.1
pH-KCl	4.3	3.6	3.9	4.2	4.6	5.5
P-Mehlich1 (mg kg^{-1})	10.2	2.0	4.0	5.0	9.3	117
Ca^{2+} ($mmol_c$ kg^{-1})	32	2	12	26	42	128
K^{+} ($mmol_c$ kg^{-1})	1.2	0.5	0.8	1.0	1.2	3.1
Mg^{2+} ($mmol_c$ kg^{-1})	10	1	5	9	12	36
Al^{3+} ($mmol_c$ kg^{-1})	9	2	2	5	14	29
Exchangeable acidity (%)	59	26	49	59	70	102
CEC ($mmol_c$ kg^{-1})	102	48	86	96	113	197
Base saturation (%)	39	4	24	39	53	87

* The real A-horizon depth is deeper in some sampling points since only the upper 20 cm were sampled.

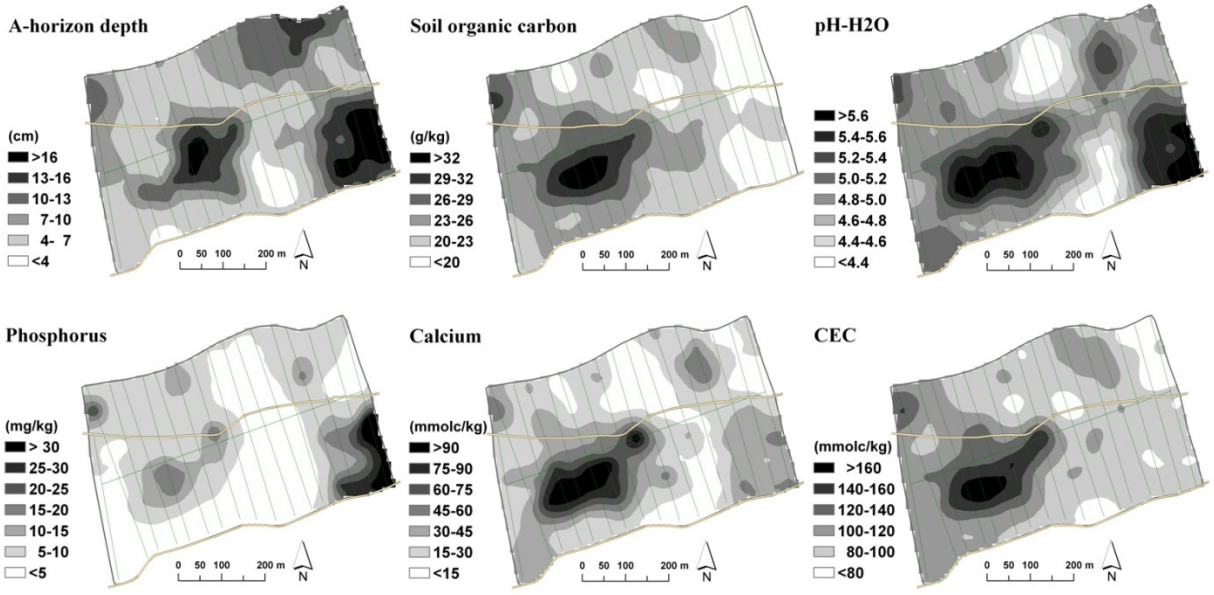

Fig. 2. Interpolated maps of soil properties normally used as indicators of ADE soils.

The average Mehlich soluble P concentration is 10 mg kg^{-1}. Values are highest around homesteads, present and past, indicating influence from P-rich kitchen waste, bones in particular. However, only three samples had P concentrations above the 65 mg kg^{-1} (the value refers to the same extraction method as we used) threshold that Kämpf et al. (2003) suggest as the limit for an anthropopedogenic horizon. The anthropogenic soil profile in the excavated settlement area have P concentrations up to 350 mg kg^{-1} in the 53 cm deep hortic A-horizon. The high phosphorus level in the arable field is probably mainly due to P fertilization. P levels are very low in areas not clearly influenced by human activities. This is characteristic for the strongly weathered Ferralsols that dominate the area. These are poor in P and have a great capacity to adsorb P in a form not readily available to plants. This adsorption capacity increases the lower the soil pH.

The spatial variation in CEC largely reflects the variation in C content, indicating that most of the CEC can be ascribed to negative charges on organic matter and charcoal. Data from the sample sites with the lowest organic matter content and from deep horizons in soil profiles presented in Araújo (2012) indicate a CEC of less than 50 $mmol_c$ kg^{-1} of soil not influenced by human activities. Calcium is the dominating cation in soils with pH-H_2O of 5.0 and higher. In more acid and usually less C-rich soils Al^{3+} is the dominating cation. Al^{3+} takes over the exchange

complex when its solubility increases at low pH. Thus, the spatial variation in Al^{3+} is largely a mirror image of the variation in pH. There is also a very close correlation between pH and base saturation. The base cations Ca^{2+}, Mg^{2+} and K^{+} tend to be highest where C content is highest, a reflection of higher CEC and less competition from Al^{3+} due to higher pH at those locations. In the arable field the concentration of K is high despite a fairly low CEC, indicating inputs from fertilization. The Ca in the anthropogenic soils may have been supplied from bones. The calcium carbonates in bones probably also have had a lime effect in anthropogenic soil layers.

Sensor mapping

The variogram parameters for the sensor data are shown in Table 2. One measure of the stability of the spatial variation is the nugget/sill ratio ($C_0 (C_0+C)^{-1}$ in the table). In this case, the high value for Th (55%) reveals that the short range variation is substantial, and a resulting map will be relatively uncertain and will vary much less than the observations. This ratio was also relatively high for MSa (35%). The ECa data was the most stable with a zero nugget. The fitted spherical variograms imply a smoother short range variation (ECa and MSa) as compared with the exponential model (TC and Th). The appearance of the resulting sensor maps (Fig. 3) is reflected by the variogram parameters. The nugget variance of the gamma variables K and U constituted 100% of the total variance, meaning that the spatial variation is totally random and interpolation is not meaningful.

Table 2. Parameters for the isotropic model variograms fitted to the sample variograms used for mapping sensor variables electrical conductivity (ECa), magnetic susceptibility (MSa), thorium concentration (^{232}Th) and total gamma counts (TC).

Variable	Variogram model	Nugget C_0 (unit^2)	Partial sill C (unit^2)	$C_0 (C_0+C)^{-1}$ (%)	Range a* (m)
ECa (mS m^{-1})	Spherical	0	1.36	0	300
MSa (ppt)	Spherical	0.49	0.92	35	177
TC (counts s^{-1})	Exponential	478	2218	18	252
^{232}Th (Bq kg^{-1})	Exponential	49.9	40.8	55	161

* Effective range $a = 3R$ in case of exponential model and $a = R$ if spherical, where R is the distance parameter.

Maps for TC, ECa and MSa are shown in Figure 3. The arable field in the southeast corner of the study area clearly deviates substantially from the rest of the area, with the highest sensor values of all parameters except for MSa, which is low in that part. The current homestead area in the northeast is also relatively high in ECa and TC, and in this case very high in MSa.

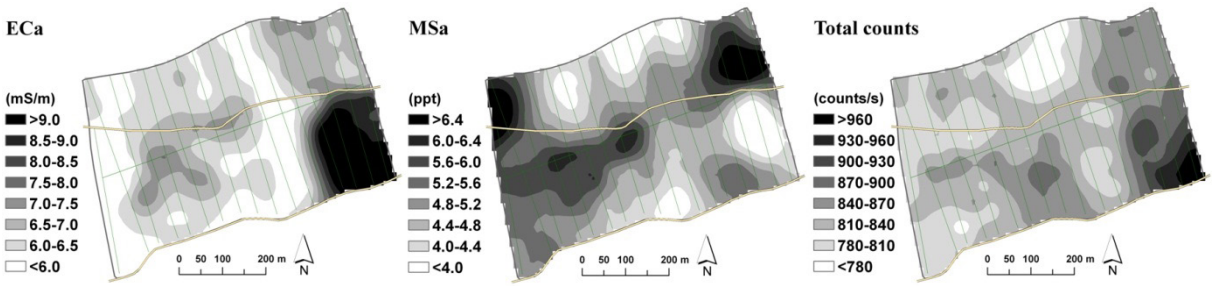

Fig. 3. Interpolated maps of electrical conductivity (ECa), magnetic susceptibility MSa and total gamma counts (TC).

Fuzzy classification

A visual comparison between the maps of soil properties (Fig. 2) and sensor data (Fig. 3) indicates that mainly ECa and MSa capture the central part of the forest where the mapped soil properties have the highest values. Fuzzy *k*-means clustering was used to combine and classify the sensor data. The lowest FPI (0.206) was achieved when $q = 1.3$ and with five classes. The centre combination of the sensor Z-scores for each class is shown in Table 3. Fuzzy class a contains the highest Th values and high TC, but relatively low ECa and MSa. Class b is high in TC, but has the lowest Th and MSa, and low ECa. Class c has the lowest TC and ECa, but fairly high MSa and average Th. Class d has average gamma values, but the lowest MSa and relatively high ECa. In Class e data measured by the EMI instrument were on average >1.5 standard deviations higher than the mean. However, for the gamma data (TC and Th) the values in class e are more moderate.

Table 3. Class centres of sensor Z-scores for five fuzzy k-means classes.

Class	TC	Th	ECa	MSa
a	1.09	1.34	-0.30	-0.16
b	1.00	-1.24	-0.29	-0.61
c	-0.41	-0.04	-0.69	0.57
d	0.07	-0.11	0.61	-0.77
e	0.96	0.43	2.08	1.51

Disregarding the disturbed easternmost samples from further assessment we compared how a number of pertinent ADE indicators displayed in Figure 2 (depth of A horizon, C, pH, Ca, P and CEC) varied between the different fuzzy classes (Fig. 4). In this case, the maximum class membership of each observation point was used in the stratification of the data. Class e contained by far the highest values of all these soil variables. For the other classes a–d, the soil variables have in general only small differences between classes. But the range of values in each class was quite large, which indicates that there are soil observations within most classes that deviate substantially from the mean or median value of the sensor class. For example, class d includes a few high values of P and also C, although the major bulk of data (25–75 percentile) does not overlap those of class e. This sensor classification seems to be working well for depicting the soil class high in nutrients and carbon.

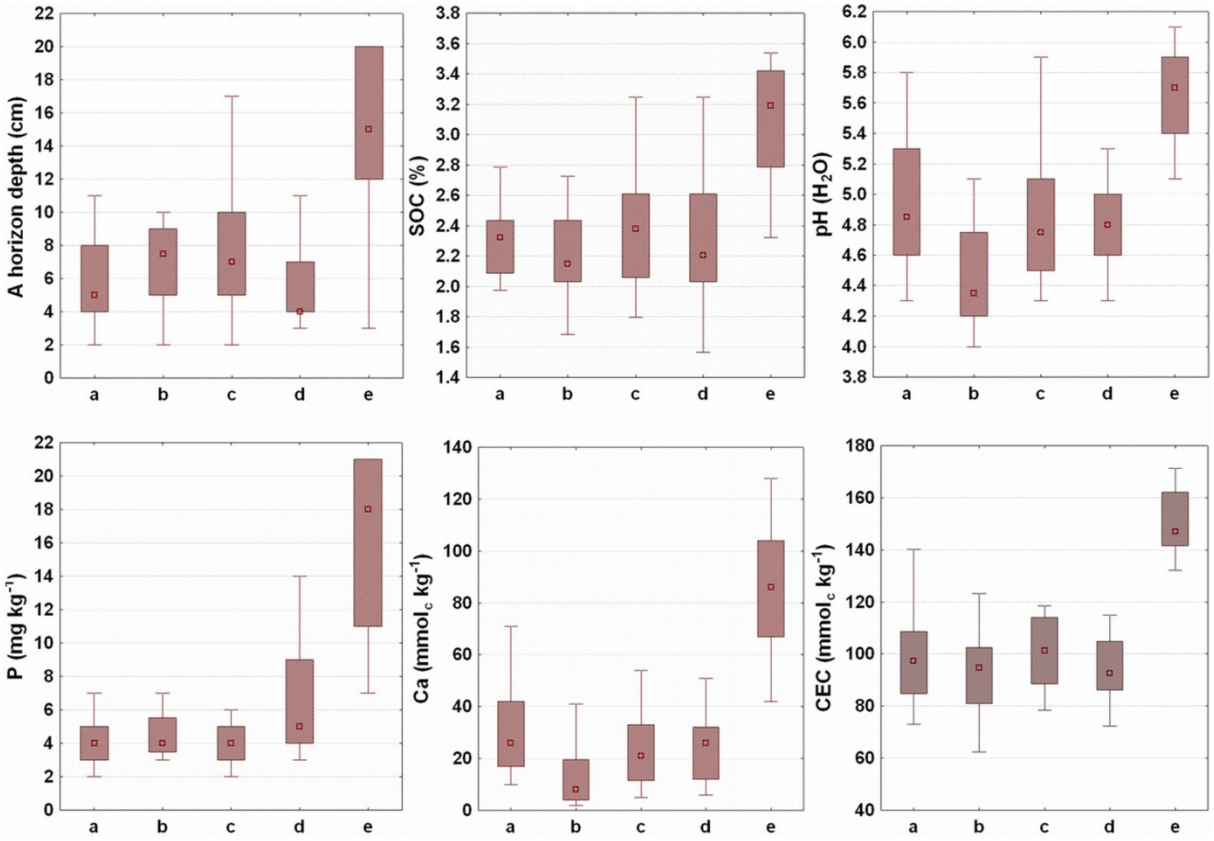

Fig. 4. Box plots of soil variables typically indicating ADE soils versus sensor fuzzy classes a–e. The box = 25–75 percentiles, the mark = median and the whiskers indicate non-outlier range (as defined by Hill and Lewicki 2007). The number of soil analyses in the different classes was: a = 18, b = 16, c = 28, d = 19, e = 9.

Membership values for class e was interpolated using kriging, producing an estimate of the likelihood that a location belongs to this class. The variogram (spherical model variogram; C_0 = 0001, C_0+C = 0.1, R = 160 m) is shown to the right in Figure 5. The resulting map is displayed to the left in Figure 5. According to this map only a small area is likely to belong to class e. Those soils are found in a crescent-shaped area where the archaeological excavations took place; a good indicator of the occurrence of ADE. Another, circular area in the centre is also portrayed as belonging to class e. In the northwest, close to a homestead, soils could with some likelihood belong to class e as well.

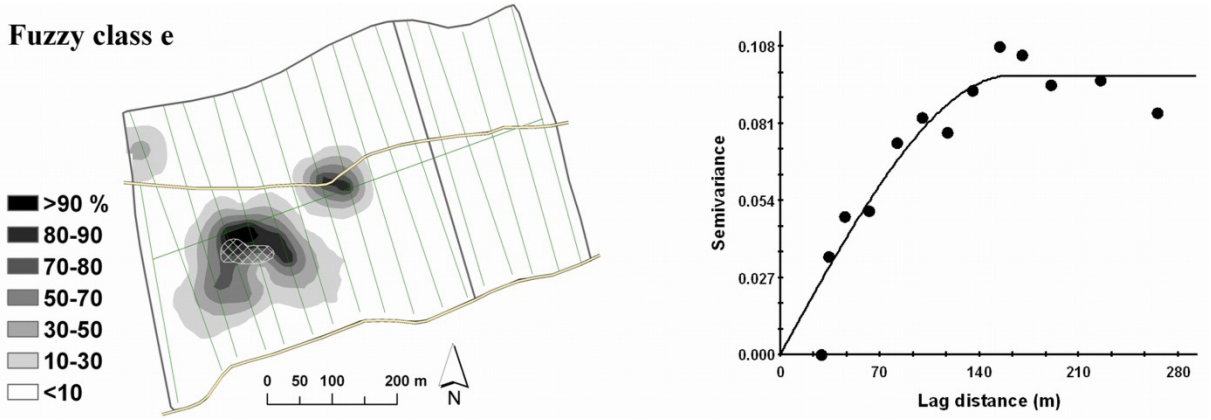

Fig. 5. Left: Likelihood to belong to fuzzy soil class e. The current archaeological excavation area is crosshatched. Right: Experimental variogram of membership to fuzzy class e with the best fitting (spherical) model.

Discussion

Although the satellite positioning of sensor registrations along transects in dense vegetation was not accurate enough to allow a direct comparison between soil observations and sensor data, the results indicate that in particular the EMI sensor is useful for mapping ADE indicators. Comparing Figures 2 and 3, it is evident that the EMI data to some extent correlates with soil properties, whereas the TC does not follow the same spatial pattern. When all sensor data were combined in the fuzzy *k*-means classification it was possible to target the soil high in properties typical for ADE. MSa has been used as an indicator of frequent burning in archaeological contexts (e.g. Tite and Mullins 1971, Jordanova et al. 2001). Heating of soil transforms some iron oxides (haematite) to the easily magnetized minerals magnetite or maghaemite, and high soil magnetic susceptibility is a good indicator of various burning activities associated with intense occupation over a long period of time. As is shown in Figure 3b, both current homesteads in the study area as well as the area of the excavated settlement have high MSa values, but MSa is also elevated in some other sectors. Since slash-and-burn cultivation is likely to result in high soil MSa, recent forest clearing and burning can be one reason for the short-range variability of MSa. More or less the entire research area is subjected to this type of management, or has been in the recent past. To date these readings requires archaeological excavation.

A general source of instability in the sensor values is the scanning method. It is important to hold the sensors at a constant height above the ground since the response functions are non-linear and the response depth of the different sensors will change if the instrument height changes, and consequently the sensor values. Transects pass through relatively flat terrain, but there was a lot of vegetation left in some parts which made it difficult to do measurements at a constant height throughout. Different sensors are affected differently by this. The sensitivity to height variations of MSa measured by the EM38 has been reported earlier (Clay 2006). ECa is less sensitive and the values from Bom Futuro were also fairly stable, resulting in low nugget and a map with low estimation uncertainty. Areas where both ECa and MSa were high coincided with the areas where soil observations signify the occurrence of anthropogenic influence through burning as well as deposition of household waste and other organic debris, which would yield soils high in e.g. C, P, Ca and CEC. In some parts, ECa values were still elevated, but MSa very low (Class d). Elevated P but moderate C may imply some anthropogenic influence such as deposition of organic waste, but without excessive burning. As used in the present study, the gamma ray sensor seemed to be less useful for distinguishing activity areas in these strongly weathered soils. The TC map showed some relationship with the variation of the EMI sensors and the maps of the soil properties. A more productive alternative measuring technique may be to scan for a longer period at selected locations instead of continuously recording data by field walking. The latter technique would of course eventually result in a spatially more detailed prediction map. The potential to combine these with a combination of these scanning techniques is of interest for further evaluation.

The fact that the EMI variables are able to pick-up relatively weak signatures is very promising indeed for using this technique to identify patches of ADE over large areas and in heavily vegetated terrain with low surface visibility in both *terra firme* and *várzea* environments. In order to quantify ADE properties, calibration soil analyses

are still needed. Therefore, it would be highly beneficial if some rapid and cheap methods could be developed for this purpose. Successful calibrations for soil carbon content and other soil properties in the Bom Futuro study area using hyperspectral laboratory equipment (NIR/MIR spectroscopy) are reported elsewhere (Araújo 2012). We suggest that fusing of data from various sensor types such as EMI and NIR/MIR spectroscopy should be tested and evaluated further for quantitative and qualitative assessments of ADEs.

In traditional farming as well as in rapidly expanding mechanized agriculture the occurrence of ADE is of great interest due to its higher fertility compared with the dominating soils on the Belterra Plateau. In our study area situated on *terra firme* it appears as if ADEs may be less extensive and less distinct in character than those closer to *várzea* environments, which have formed the model for archaeo-pedological definitions of these kinds of soil and that may also have a different soil parent material. Few of the soils in our sampling grid fulfil the criterion for depth of a hortic horizon (20 cm; WRB, 2006). Most of the soils high in P are on the arable field and the high concentrations are obviously due to recent fertilization. For P we cannot directly compare with the criteria for a hortic horizon since those refer to extraction in sodium bicarbonate (Olsen method). However, Kämpf et al. (2003) suggested a Mehlich 1 P concentration of 65 mg kg^{-1} as the limit in their tentative definition of an archaeo-anthropedogenic horizon of an ADE. Only three sites in our grid had a concentration above these values at 0–20 cm depth. A few more sites may also have had values above the limit if only the A-horizon would have been analysed separately. However, description and analysis of excavated profiles indicate that there are soil patches of ca. 100 m^2 clearly affected by ancient domestic activities: (e.g. carbon and ash from hearths, deposition of food remains and excrements) that have an A-horizon around 50 cm in depth that fulfil the criteria for a hortic horizon, as well as most of the criteria that Kämpf et al. (2003) suggest for an archaeo-anthropedogenic horizon. These soils could definitely be referred to as *terra preta*. Some of the other anthropogenic soils in the area are probably better termed *terra mulata*. However, further studies should be carried out to determine how representative our initial observations at Bom Futuro are and to better understand the extent of ADE formations in *terra firme* environments. In our present understanding of prehistoric settlement in the Amazon, less intense signatures is to be expected since long-term settlement appears to have been concentrated along the main waterways whereas *terra firme* uplands were occupied relatively late, a few centuries before European contact.

In conclusion, soil properties typical for ADE such as SOC, P, CEC and Ca showed a relatively consistent spatial pattern in the test study at Bom Futuro, notwithstanding that the concentrations in the studied upland area in general were lower than in areas with more prominent ADE soils. Proximal soil sensing and fuzzy classification could be used for delineating areas with the highest concentrations of these soil properties. The sensor parameters ECa and MSa as measured by the EMI instrument were good indicators of these soil properties, but the gamma radiation sensor was less useful in the strongly weathered soils of the study area.

Acknowledgements

This research was conducted as part of the project 'Cultivated Wilderness,' financed by a grant from the Bank of Sweden Tercentenary Foundation. Field research permission was granted by Conselho Nacional de Desenvolvimento Científico e Tecnológico (CNPq) and Instituto do Patrimônio Histórico e Artístico Nacional (IPHAN). Marcio Amaral provided valuable field and logistical support. We are indebted to local land owners and managers, particularly Manoel Feliciano Costa, for hospitality and permission to work at Bom Futuro.

References

Adamchuk, V.I. & Viscarra Rossel, R.A. 2013. Special issue on soil sensing. *Geoderma* 199:1.

Burrough, P.A. & McDonnell, R.A. 1998. *Principles of geographical information systems*. Oxford: Oxford University Press. 356 p.

Araújo, S.R. 2012. *Reflectance spectroscopy vis-NIR and mid-IR applied for soil studies*. Unpublished PhD thesis. University of São Paulo, College of Agriculture "Luiz de Queiroz", Piracicaba, Brazil. 174 p.

Clay, R.B. 2006. Conductivity survey: a survival manual. In: Johnson, J.K (ed.). *Remote sensing in archaeology: an explicitly North American perspective*. Tuscaloosa: University of Alabama Press. p. 79–108.

Corwin, D.L. & Lesch, S.M. 2003. Application of soil electrical conductivity to precision agriculture: theory, principles, and guidelines. *Agronomy Journal* 95: 455–471.

EMBRAPA 2009. *Sistema brasileiro de classificação de solos*. 2nd ed. Rio de Janeiro: EMBRAPA. 306 p.

FAO 1988. *FAO/Unesco soil map of the world*. Revised legend. World Soil Resources Report 60. Rome: FAO. 109 p.

Fearnside, P.M. & Leal Filho, N. 2001. Soil and development in Amazonia: lessons from the biological dynamics of forest fragments project. In: Bierregaard, R.O., Gascon, C., Lovejoy, T.E. & Mesquita, R.C.G. (eds.). *Lessons from Amazonia: the ecology and conservation of a fragmented forest*. New Haven: Yale University Press, p. 291–312.

Glaser, B. & Birk, J.J. 2012. State of the scientific knowledge on properties and genesis of Anthropogenic Dark Earths in Central Amazonia (terra preta de Índio). *Geochimica Et Cosmochimica Acta* 82: 39–51.

Glaser, B. & Woods, W.I. (eds.). 2004. *Explorations in Amazonian Dark Earths*. Berlin: Springer. 212 p.

Grunwald, S. 2010. Current state of digital soil mapping and what is next? In: Boettinger, J.L., Howell, D.W., Moore, A.C., Hartemink, A.E. & Kienast-Brown, S. (eds.). *Digital soil mapping. Progress in Soil Science 2*. Berlin: Springer. p. 3–12.

Hartt, C.F. 1874. Contributions to the geology and physical geography of the lower Amazonas. *Bulletin of the Buffalo Society of Natural Sciences* 1: 201−235.

Hendriks, P.H.G.M., Limburg, J. & de Meijer, R.J. 2001. Full-spectrum analysis of natural gamma-ray spectra. *Journal of Environmental Radioactivity* 53: 365–380.

Hill, T. & Lewicki, P. 2007. *Statistics: methods and applications*. Tulsa, USA: StatSoft. 800 p.

IAEA 2003. *Guidelines for radioelement mapping using gamma ray spectrometry data*. IAEA-TECDOC-1363. Vienna: IAEA. 173 p.

Irion, G. 1984, Clay minerals of Amazonian soils. In: Sioli, H. (ed.). *The Amazon: limnology and landscape ecology of a mighty tropical river and its basin*. Monographie biologicae, vol. 56. Dordrecht: Dr W. Junk Publishers. p. 537–580.

Isaaks E.H. & Srivastava, R.M. 1989. *An introduction to applied geostatistics*. New York: Oxford University Press. 592 p.

Jordanova, N., Petrovsky, E., Kovacheva, M. & Jordanova, D. 2001. Factors determining magnetic enhancement of burnt clay from archaeological sites. *Journal of Archaeological Science* 28: 1137–1148.

Kämpf, N., Woods, W.I., Sombroek, W.G., Kern, D.C. & Cunha, T.J.F. 2003. Classification of Amazonian dark earths and other ancient anthropic soils. In: Lehmann, J., Kern, D.C., Glaser, B. & Woods, W.I. (eds.). *Amazonian Dark Earths: origin, properties, management*. Dordrecht: Kluwer. p. 77–102.

Lehmann, J. & Joseph, S. 2009. *Biochar for enviromental management*. Sterling, USA: Earthscan Publishing. 448 p.

Lehmann, J., Kern, D.C., Glaser, B. & Woods, W.I. (eds.). 2003. *Amazonian Dark Earths: origin, properties, management*. Dordrecht: Kluwer. 524 p.

Minasny, B. & McBratney, A.B. 2002. *FuzME version 3.0*. Sydney: Australian Centre for Precision Agriculture.

Nimuendajú, C. 2004. *In Pursuit of a Past Amazon: Archaeological Researches in the Brazilian Guyana and in the Amazon Region*. Stenborg, P. (ed.). Etnologiska Studier 45. Gothenburg: Världskulturmuseet. 380 p.

Piikki, K., Söderström, M. & Stenberg, B. 2013. Sensor data fusion for topsoil clay mapping. *Geoderma* 199: 106–111.

Smith, N.J.H. 1980. Anthrosols and human carrying capacity in Amazonia. *Annals of the Association of American Geographers* 70: 553–566.

Söderström, M. & Eriksson, J. 2013. Gamma-ray spectrometry and geological maps as tools for cadmium risk assessment in arable soils. *Geoderma* 192: 323–334.

Sombroek, W. 1966. *Amazon soils: a reconnaissance of the soils of the Brazilian Amazon Region*. Wageningen: Center for agricultural publishing and documentation. 292 p.

Stenborg, P. 2009. Points of convergence — routes of divergence: Some considerations based on Curt Nimuendajú's archaeological work in the Santarém–Trombetas area and at Amapá. In: Whitehead, N.L. & Alemán, S.W. (eds.). *Anthropologies of Guayana: Cultural Spaces in Northeastern Amazonia*. The University of Arizona Press. p. 55–73.

Stenborg, P. & Bakunic, I. 2011. S*econd Report from the project Material Culture and Change in the Lower Amazon*. Gothenburg: GOTARC. Serie D, Arkeologiska rapporter nr 83. Gothenburg University. 23 p.

Stenborg, P.,Schaan, D. & Amaral Lima, M. 2012 Precolumbian land use and settlement pattern in the Santarém Region, lower Amazon. *Amazônica - Revista de Antropologia*, 4: 222-250.

Teixeira, W.G., Arruda, W., Lima, H.N., Iwata, S.A. & Martins, G.C. 2008. Building a digital soil data base of the Solimões river region in the Brazilian Central Amazon. In: Hartemink, A.E., McBratney, A.B. & Mendonça-Santos, M.L. (eds.). *Digital soil mapping with limited data*. Berlin: Springer. p. 327–335.

Tite, M.S. & Mullins, C. 1971. Enhancement of the magnetic susceptibility of soils on archaeological sites. *Archaeometry* 13: 209–219.

van der Klooster, E., Van Egmond, F.M. & Sonneveld, M.P.W. 2011. Mapping soil clay contents in Dutch marine districts using gamma-ray spectrometry. *European Journal of Soil Science* 62: 743–753.

Verheijen, F., Jeffery, S., Bastos, A.C., van der Velde, M. & Diafas, I. 2010. *Biochar application to soils. A critical scientific review of effects on soil properties, processes and functions.* Ispra, Italy: European Commission, Joint Research Centre, Institute for Environment and Sustainability. 166 p.

Viscarra Rossel, R.A. & McBratney, A.B. 1998. Laboratory evaluation of a proximal sensing technique for simultaneous measurement of soil clay and water content. *Geoderma* 85: 19–39.

Woods, W.I. & McCann, J.M. 1999. The anthropogenic origin and persistence of Amazonian Dark Earths. In: Caviedes, C. (ed.) Y*earbook 1999—Conference of Latin Americanist Geographers*. Austin: University of Texas Press. 25: 7–14.

Woods, W.I, Teixeira, W.G., Lehmann, J., Steiner, C., WinklerPrins, A.M.G.A. & Rebellato, L. (eds.). 2009. *Amazonian Dark Earths: Wim Sombroek's vision*. Berlin: Springer. 502 p.

WRB 2006. *World reference base for soil resources 2006. A framework for international classification, correlation and communication*. World Soil Resources Report 103. Rome: FAO. 128 p.